# Atomic scattering as a probe of polymer surface and thin film dynamics

M. A. Freedman, A. W. Rosenbaum, and S. J. Sibener*
*The James Franck Institute and Department of Chemistry, The University of Chicago, 929 East 57th Street, Chicago, Illinois 60637, USA*

(Received 30 January 2007; published 29 March 2007)

Collisional energy transfer at the surface of poly(methyl methacrylate) thin films on $SiO_x$/Si was investigated using low-energy neutral helium atom scattering. Analysis of spectra in two scattering regimes yields results consistent with the hypothesis that thinner films are stiffer, suggesting that for highly nanoconfined films, polymer-substrate interactions influence vibrational dynamics at the polymer-vacuum interface. Specifically, thinner films are found to have lower mean-square displacements and decreased annihilation events as compared to thicker films. The scattering spectra are fit well by a semiclassical scattering model, though deviations arise at sample temperatures near the bulk glass transition. We have found helium atom scattering to be a sensitive probe of the vibrational dynamics of the polymer thin film surface. This technique holds promise for the exploration of glassy dynamics of polymer thin films.

DOI: 10.1103/PhysRevB.75.113410 PACS number(s): 79.20.Rf, 81.05.Lg, 82.20.−w, 64.70.Pf

Collisional energy transfer at the gas-surface interface has been widely studied for several decades,[1] but only recently has information on complex interfaces been obtained.[2,3] Studies of complex interfaces are of great interest due to their applications in material, environmental, and combustion science, among other fields. One area of interest is the effect of nanoconfinement and surface behavior on polymer properties.[4] Researchers have characterized polymer surfaces using a variety of methods.[5,6] Of particular interest is how vibrational motion at the polymer thin film surface affects the surface and overall glass transition.[7] Molecular beam methods were seminal in the investigation of vibrational and diffusional motion of atomic and diatomic adsorbates on clean single-crystal surfaces. Recent work expanding these studies to more complex systems indicates potential for the investigation of polymer thin films.

In this paper, we directly probe the surface dynamics of poly(methyl methacrylate) (PMMA) thin films at the polymer-vacuum interface using low-energy neutral helium atom scattering. This technique is more highly surface sensitive and nonperturbative[8] than previous methods used to study polymer surfaces. Even neutron and x-ray scattering techniques probe the selvedge region rather than the topmost interfacial layer. We have characterized the vibrational dynamics of PMMA using elastic and inelastic scattering as a function of film thickness and temperature to gain insight into movement at the topmost interfacial layer. We have also investigated the influence of nanoconfinement in molecularly thin polymer films on collisional energy transfer.

Experiments were conducted in a high momentum- and energy-resolution helium atom scattering apparatus. Elastic and inelastic scattering events can be observed through diffraction and time of flight (TOF), respectively. This instrument has been described in detail elsewhere; its design will only be summarized here.[9,10] It consists of a cryogenically cooled supersonic helium beam source and an ultrahigh-vacuum (UHV) scattering chamber with a rotating, long-flight-path (sample to ionizer distance of 1.005 m) quadrupole mass spectrometer detector. The angular collimation yields a resolution of 0.22°, and the $\Delta v/v$ for most beam energies used is less than 1%. A cross-correlation time-of-flight technique with a pseudorandom chopping sequence is used to maximize signal to noise.[11]

We spin high molecular weight, monodisperse, atactic PMMA ($M_w$=350 kg/mol and $M_w/M_n$=1.15, PolySciences) on $SiO_x$/Si(100) substrates. The films were annealed at 413 K for 120 min. In this experiment we spun films that were approximately 10 nm or 50 nm thick, as measured *ex situ* by ellipsometry. Using 15 nm for the radius of gyration, $R_g$, as found for PMMA of similar molecular weight at the $\theta$ condition,[12] our samples were $0.67R_g$ and $3.3R_g$ thick, respectively. Optical microscopy and atomic force microscopy were used to further assess the uniformity of the film. Samples were inserted in the scattering chamber (base pressure of $10^{-10}$ to $10^{-9}$ torr) and annealed at the beginning of each experimental run at 440 K for 30 min. The samples were subsequently cooled to the lowest temperature used and spectra for various ascending temperatures were taken, using heating rates of 5 K/min. Changes to the cooling rate did not affect the results. From thermogravimetric analysis, the PMMA sample begins to degrade at temperatures above approximately 550 K in a nitrogen atmosphere. Scattering experiments were therefore not performed at temperatures above 490 K.

We obtained spectra for a wide range of parameters in specular and nonspecular geometries. In the specular geometry, experiments were performed at angles of 24.42°, 32.42°, and 37.42°, for beam energies from 9.7 meV to 54 meV (4.31 Å$^{-1}$ with $\Delta K$=1.76 Å$^{-1}$ to 10.15 Å$^{-1}$ with $\Delta K$=4.16 Å$^{-1}$) and sample temperatures from 60 K to 490 K. The scattering results were highly reproducible.

At cryogenic beam energies and sample temperatures, an elastic feature was observed in the TOF spectra. Figure 1 shows TOF spectra for a 10.6 nm thick PMMA film at sample temperatures between 60 K and 120 K. The elastic peak decays slightly faster for the thicker films, but in neither case is it discernable from the diffuse scattering signal by 150 K. This feature does not decay over a parallel momentum range of 2.0 Å$^{-1}$, suggesting that this feature may be a diffuse rather than a coherent elastic peak.

Representative TOF spectra taken in the specular geom-

 

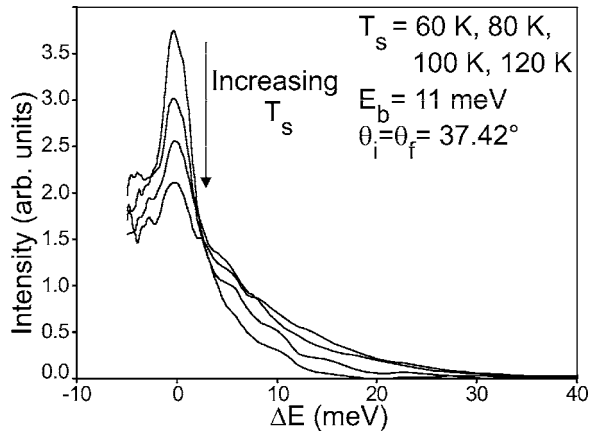


FIG. 1. Elastic scattering observed for a 10.6 nm film with a 11 meV beam, sample temperatures of 60, 80, 100, and 120 K, and incident and final angles of 37.42°.

etry for sample temperatures of 200 K to 490 K and beam energies from 9.7 meV to 54 meV are shown in Fig. 2. A spectrum of HOPG graphite is shown for comparison. The HOPG graphite spectrum arises due to elastic scattering and is narrower than the broad asymmetric curve from PMMA. Note that the intensity of the curve decreases with increasing temperature. The position of the intensity maximum shifts to higher $\Delta E$ and the high-energy tail grows as the temperature increases, as expected due to an increase in annihilation contributions to the collisional energy transfer. These trends are observed regardless of sample thickness, beam energy, and scattering geometry. As the beam energy increases, the spectra span a greater range of $\Delta E$.

The mean-square displacement of the PMMA surface can be determined from the Debye-Waller factor derived from the elastic feature. The elastic intensity decreases exponentially with a temperature-dependent factor of $2w$, the Debye-Waller factor. The equation $2w=\Delta k_z\langle u_z^2\rangle+\Delta k_\parallel\langle u_\parallel^2\rangle$ links the Debye-Waller factor to the momenta $\Delta k_z$ and $\Delta k_\parallel$ and the

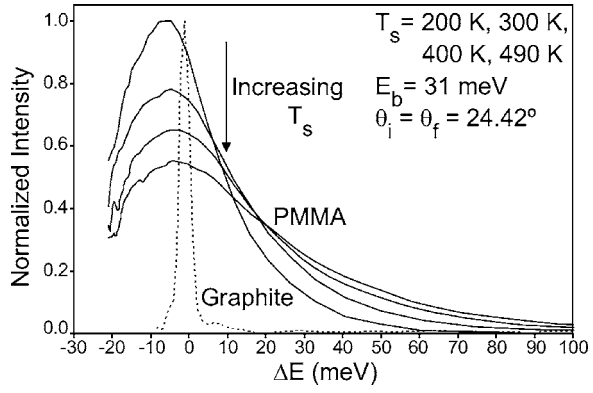


FIG. 2. Multiphonon scattering for a 10.6 nm thick film with a beam energy of 31 meV, sample temperatures of 200, 300, 400, and 490 K, and incident and final angles of 24.42°. The dashed line is a spectrum of HOPG graphite at 300 K with a beam energy of 14 meV and initial and final angles of 37.42°. The graphite reflectivity is significantly more intense than from the disordered, softer PMMA surface.

mean-square displacements $\langle u_z^2\rangle$ and $\langle u_\parallel^2\rangle$ normal and parallel to the surface, respectively. Due to the specular geometry, only $\langle u_z^2\rangle$ was found. Because the inelastic background contributes approximately equally to the area of the elastic peak over this narrow temperature range, the amplitudes were used to calculate $2w$, but deconvolution of the features yields similar results. The Debye-Waller plot gives a $\langle u_z^2\rangle$ value of $6.0\pm0.5\times10^{-5}$ Å$^2$/K for the 10 nm film and $6.9\pm0.5\times10^{-5}$ Å$^2$/K for the 50 nm film. The suppression in mean-square displacement of the thinner samples agrees qualitatively with neutron scattering results[6] and most likely is due to increased interaction with the substrate. Similarly, in helium atom scattering studies of alkanethiol self-assembled monolayers (SAMs) on Au(111), a larger mean-square displacement was found for longer chain lengths.[2,13] It is interesting that the values calculated for PMMA films are the same order of magnitude as found for the low-density phase of alkanethiol SAMs on Au(111).[2] Helium atom scattering therefore predicts intrinsic differences in the mean-square displacement of films of varying thicknesses even at the lowest sample temperatures.

The spectra for a given film thickness depend on the scattering geometry. The spectra taken in the specular geometry broaden on the annihilation side as the scattering angle becomes more normal. The resultant increase in the perpendicular component of the momentum can lead directly to the result obtained through increased energy transfer or, indirectly, by increasing the propensity for multiple scattering events (for example, see Ref. 14). The orientation of the film can also affect the scattering spectra, as in the case of SAMs where head-on collisions result in less efficient energy exchange.

The spectra of the thicker films have a more pronounced dependence on the scattering geometry than the spectra of the thinner films (Fig. 3). At 37.42°, the inelastic spectra can be superimposed for the 10 nm and 50 nm samples, but as the scattering angle gets closer to normal, the thicker film displays more annihilation events. The difference between the thicknesses is robust and is largest for the highest sample temperatures. At least two processes are hypothesized to contibute to this difference: interaction with the substrate and molecular coarsening of the interface due to an increase in thermal motion. The reduction in annhilation events observed for the 10 nm films may arise from a stronger interaction with the substrate, making the surface stiffer. Rare gas scattering studies of liquids and organic monolayers have shown the sensitivity of scattering on the ratio of the mass of the gas to the mass of the surface.[15] The liquid-vacuum interface coarsens on a molecular level as the surface temperature is increased due to thermal motion.[16] In Fig. 2, the widths of the spectra for a single film thickness increase as the surface temperature rises, indicating a greater degree of thermal motion of the surface layer. The temperature dependence plots in Fig. 3 demonstrate how the surfaces change with respect to each other. Because the difference between the spectra increases with temperature, the 50 nm films appear to coarsen slightly more than the 10 nm films, which is consistent with the idea that the thinner films are stiffer. These results further demonstrate the sensitivity of helium

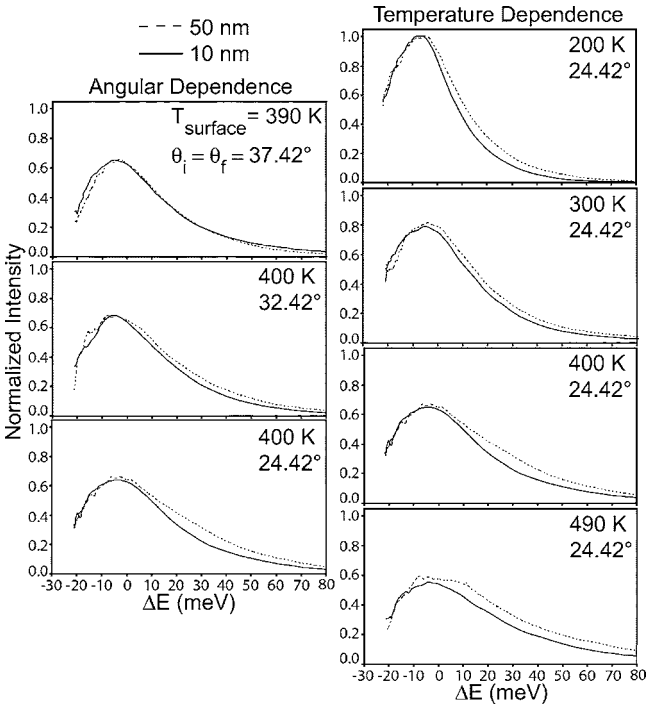


FIG. 3. The angular (left panels) and temperature (right panels) dependence of the inelastic spectra on film thickness for spectra taken in the specular geometry at a beam energy of 31 meV. At angles closer to normal, the 46.6 nm film (dashed line) has a larger high $\Delta E$ tail than the 10.6 nm (solid line) film. The difference observed as a function of the film thickness is robust over a wide range of surface temperatures.

atom scattering to intrinsic differences that arise due to film thickness.

We used a semiclassical model developed by Manson, Celli, and Himes[17] to fit the inelastic line shape for the spectra taken at beam energies at and above 30 meV. Two different models were developed, one in which scattering occurs from a continuum of atomic centers and one from discrete atomic centers.[18] The former has been used for single crystal metal surfaces and the latter for a fatty acid monolayer. In the continuum model, the intensity of the multiphonon spectra decreases with temperature according to $(\hbar\omega_0 k_B T_S)^{-3/2}$, where $\hbar\omega_0$ is the classical recoil velocity and $T_S$ is the surface temperature. For the discrete model, the temperature dependence is $(\hbar\omega_0 k_B T_S)^{-1/2}$. We have used the Baule approximation for $\hbar\omega_0$.[18] Figure 3 demonstrates that the decay of the maximum intensity is the same for both film thicknesses. Figure 4 shows that the temperature dependence of the discrete model fits the temperature decay of our data, whereas the continuum model decays too rapidly. The parameters for the PMMA system are the surface mass $M$, the He-surface well depth $D$, the nondimensionalization factor for the perpendicular momentum $\beta$, and the parallel momentum cutoff factor $Q_c$. There are only two free parameters, as we fix $M$ and $D$. We assume $D$ is 10 meV, which is close to values for high-density alkanethiol SAMs.[13] Consistent with sum frequency generation (SFG) vibrational spectroscopy, helium probably interacts primarily with the terminal methyl groups on the ester methyl side chain, giving $M=15$ amu.[19]

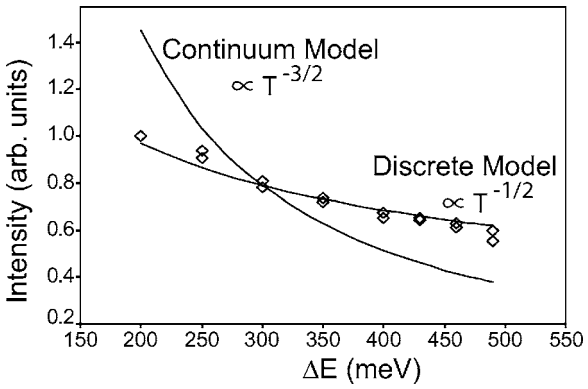


FIG. 4. The experimental intensity (◇) is compared to two semiclassical scattering models. The data were taken from 10.6 nm and 46.6 nm thick samples with a beam energy of 31 meV and incident and final angles of 27.42°. The models and data are normalized at 300 K to illustrate the difference in curvature of the two models. The data clearly follow the decay of the discrete model.

The values of $\beta$ and $Q_c$ were fixed for a given set of spectra and were generally between 2 Å$^{-1}$ and 6 Å$^{-1}$. A fit to the discrete centers model is shown in Fig. 5(a), using a form factor from Ref. 20.

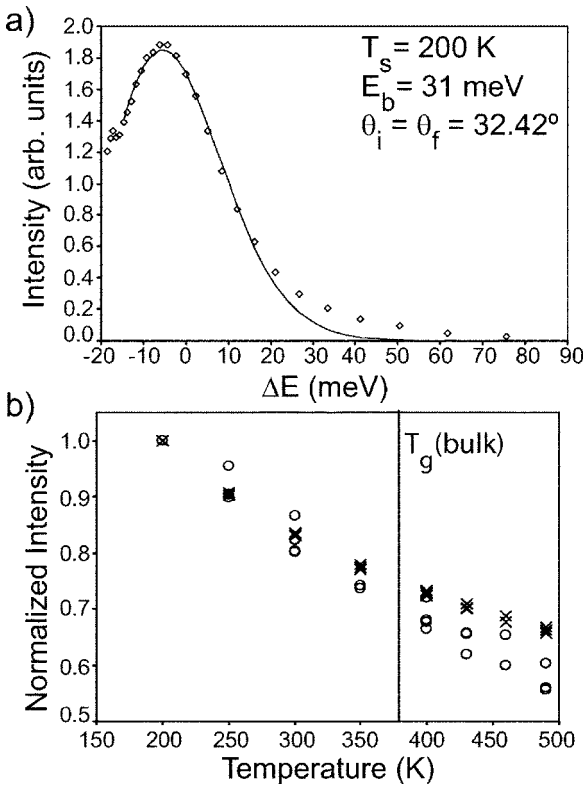


FIG. 5. (a) The discrete semiclassical model (solid line) was used to fit the 200 K spectrum (◇) on a 46.6 nm thick film with a 30.6 meV beam and incident and final angles of 32.42°. The model was propagated using the same parameter set for the higher sample temperatures. (b) The deviation of the integrated intensity between theory (×) and experiment (○) in a $|\Delta E|=10$ range around the peak maximum. The data were obtained at a beam energy of 31 meV for a variety of sample thicknesses and incident and final angles.

The model is used to fit the lowest sample temperature [Fig. 5(a)] and then propagated with the same parameter set for higher temperatures as an estimate of surface behavior. Good agreement is obtained for the fit to the 200 K spectrum except in the region of the high-energy tail because of the inclusion of only single collisions in the model. While the lower temperature spectra fit the model well, agreement between the experiment and the model breaks down before the bulk glass transition temperature of 378 K [Fig. 5(b)]. This deviation indicates that a change in the vibrational dynamics of these films arises at higher temperatures. This change could be due to increased thermal motion at temperatures above the glass transition.

In summary, we have investigated the dynamics of the polymer thin film interface with a precise and exclusively surface sensitive probe, low-energy neutral helium atom scattering. We have shown that this highly surface-sensitive and nonperturbative technique provides a novel means for exploring surface vibrational dynamics at complex interfaces. Analysis of elastic and inelastic spectra is consistent with the hypothesis that the thinner film is stiffer, emphasizing the importance of substrate-polymer interactions on the dynamics at the topmost interfacial layer. Specifically, we find thinner films to have a smaller mean-square displacement perpendicular to the surface and less efficient vibrational energy transfer in collisions with He atoms. A discrete semiclassical scattering model was also used to analyze the multiphonon spectra as a function of temperature. Deviations to the theory arise near the bulk glass transition temperature of PMMA and may indeed be due to changes in the vibrational modes at the interface of the thin film over the glass transition temperature. We hope to extend these studies to explore a range of polymer systems and further investigate glassy dynamics.

We thank J. Hinch, E. Ciftlikli, J. Douglas, C. Soles, K. Freed, G. Nathanson, and W. Hase for helpful discussions. We also thank S. Jones and Q. Zheng for sample preparation training, S. Yuan for the thermogravimetric analysis, and K. Gibson for general help. This work was primarily supported by the Air Force Office of Scientific Research. We also received funding through the NSF-MRSEC at the University of Chicago, Grant No. NSF-DMR-0213745. M.A.F. acknowledges support from the National Science Foundation.

*Electronic address: s-sibener@uchicago.edu

[1] *Dynamics of Gas-Surface Interaction*, edited by G. Benedek and U. Valbusa (Springer, New York, 1982).
[2] A. W. Rosenbaum, M. A. Freedman, S. B. Darling, I. Popova, and S. J. Sibener, J. Chem. Phys. **120**, 3880 (2004).
[3] E. V. Sitzmann and K. B. Eisenthal, J. Phys. Chem. **92**, 4579 (1988); D. Fuhrmann and Ch. Wöll, Surf. Sci. **377-379**, 544 (1997); G. M. Nathanson, Annu. Rev. Phys. Chem. **55**, 231 (2004).
[4] G. B. McKenna and M. Alcoutlabi, J. Phys.: Condens. Matter **17**, R461 (2005).
[5] J. H. Teichroeb and J. A. Forrest, Phys. Rev. Lett. **91**, 016104 (2003); W-l. Wu, S. Sambasivan, C-Y. Wang, W. E. Wallace, J. Genzer, and D. A. Fischer, Eur. Phys. J. E **12**, 127 (2003); C. J. Ellison and J. M. Torkelson, Nat. Mater. **2**, 695 (2003).
[6] C. L. Soles, J. F. Douglas, W-l. Wu, and R. M. Dimeo, Macromolecules **36**, 373 (2003).
[7] J. A. Forrest, Eur. Phys. J. E **8**, 261 (2002).
[8] J. P. Toennies, J. Phys.: Condens. Matter **5**, A25 (1993).
[9] L. Niu, D. D. Koleske, D. J. Gaspar, and S. J. Sibener, J. Chem. Phys. **102**, 9077 (1995).
[10] B. Gans, P. A. Knipp, D. D. Koleske, and S. J. Sibener, Surf. Sci. **264**, 81 (1992).
[11] D. D. Koleske and S. J. Sibener, Rev. Sci. Instrum. **63**, 3852 (1992).
[12] T. Konishi, T. Yoshizaki, and H. Yamakawa, Macromolecules **24**, 5614 (1991).
[13] N. Camillone III, C. E. D. Chidsey, G-y. Liu, T. M. Putvinski, and G. Scoles, J. Chem. Phys. **94**, 8493 (1991).
[14] M. E. King, K. M. Fiehrer, G. M. Nathanson, and T. K. Minton, J. Phys. Chem. A **101**, 6556 (1997).
[15] S. R. Cohen, R. Naaman, and J. Sagiv, Phys. Rev. Lett. **58**, 1208 (1987); M. E. Saecker, S. T. Govoni, D. V. Kowalski, M. E. King, and G. M. Nathanson, Science **252**, 1421 (1991).
[16] M. E. King, M. E. Saecker, and G. M. Nathanson, J. Chem. Phys. **101**, 2539 (1994).
[17] J. R. Manson, V. Celli, and D. Himes, Phys. Rev. B **49**, 2782 (1994).
[18] J. R. Manson and J. G. Skofronick, Phys. Rev. B **47**, 12890 (1993).
[19] J. Wang, C. Chen, S. M. Buck, and Z. Chen, J. Phys. Chem. B **105**, 12118 (2001).
[20] M. Li, J. R. Manson, and A. P. Graham, Phys. Rev. B **65**, 195404 (2002).